Acta Crystallographica Section F
Structural Biology and Crystallization Communications
ISSN 1744-3091

Crystallization and preliminary crystallographic analysis of the transpeptidase domain of penicillin-binding protein 2B from *Streptococcus pneumoniae*

Mototsugu Yamada,* Takashi Watanabe, Nobuyoshi Baba, Takako Miyara, Jun Saito and Yasuo Takeuchi‡

Pharmaceutical Research Center, Meiji Seika Kaisha Ltd, 760 Morooka-cho, Kohoku-ku, Yokohama 222-8567, Japan

‡ Present address: Food and Health R&D Laboratories, Meiji Seika Kaisha Ltd, 5-3-1 Chiyoda, Sakado, Saitama 350-0289, Japan.

Correspondence e-mail: mototsugu_yamada@meiji.co.jp

Received 22 November 2007
Accepted 7 March 2008

Penicillin-binding protein (PBP) 2B from *Streptococcus pneumoniae* catalyzes the cross-linking of peptidoglycan precursors that occurs during bacterial cell-wall biosynthesis. A selenomethionyl (SeMet) substituted PBP 2B transpeptidase domain was isolated from a limited proteolysis digest of a soluble form of recombinant PBP 2B and then crystallized. The crystals belonged to space group $P4_32_12$, with unit-cell parameters $a = b = 86.39$, $c = 143.27$ Å. Diffraction data were collected to 2.4 Å resolution using the BL32B2 beamline at SPring-8. The asymmetric unit contains one protein molecule and 63.7% solvent.

1. Introduction

Penicillin-binding proteins (PBPs) are enzymes that catalyze the polymerization of glycan chains and the cross-linking of adjacent stem peptides during bacterial cell-wall biosynthesis (Macheboeuf *et al.*, 2006). PBPs are classified into two groups: high-molecular-weight (hmw) and low-molecular-weight (lmw) PBPs. The hmw PBPs are further subdivided into class A and class B PBPs (Goffin & Ghuysen, 1998; Macheboeuf *et al.*, 2006). The hmw class A PBPs are bifunctional enzymes with transglycosylase and transpeptidase activities. The hmw class B PBPs, one of which is the subject of this report, act only as transpeptidases. The lmw PBPs generally act as DD-carboxypeptidases. To cross-link two peptidoglycan strands, a transpeptidase initially binds noncovalently to a peptidoglycan substrate called the donor strand. The active-site serine then attacks the carbonyl C atom of the C-terminal D-Ala-D-Ala peptide bond, forming an acyl-enzyme complex and releasing the C-terminal D-Ala. Finally, an amino N atom of a peptidoglycan acceptor strand attacks the carbonyl C atom of the acyl-enzyme to form a new peptide bond that cross-links the two peptidoglycan strands and releases free enzyme (McDonough *et al.*, 2002). Because β-lactam antibiotics such as the penicillins, cephalosporins and carbapenems structurally resemble the D-Ala-D-Ala stem-peptide moiety, they inhibit the transpeptidase and DD-carboxypeptidase activities of PBPs by acylating their active-site serines (Macheboeuf *et al.*, 2006).

Streptococcus pneumoniae causes community-acquired infections such as pneumonia, otitis media and meningitis; the emergence of penicillin-resistant *S. pneumoniae* strains has been reported worldwide (Jacobs, 2004). *S. pneumoniae* contains six PBPs: the hmw class A PBPs 1A, 1B and 2A, the hmw class B PBPs 2B and 2X, and the lmw PBP 3. Within and surrounding the active sites of PBPs are three conserved sequence motifs: Ser-*X*-*X*-Lys (S*XX*K), which includes the catalytic serine, Ser-*X*-Asn (S*X*N) and Lys-Thr/Ser-Gly (KT/SG) (Goffin & Ghuysen, 1998). A common mechanism of resistance to β-lactam antibiotics is the alteration of *pbp* genes that occurs upon gene rearrangement. Amino-acid mutations within and/or adjacent to the conserved sequence motifs can reduce the affinities of PBPs for β-lactam antibiotics, causing drug resistance. For *S. pneumoniae* PBPs 2X, 2B and 1A, β-lactam resistance frequently occurs (Barcus *et al.*, 1995). Sanbongi and colleagues sequenced the *pbp* genes of 40 *S. pneumoniae* clinical isolates and correlated the presence of

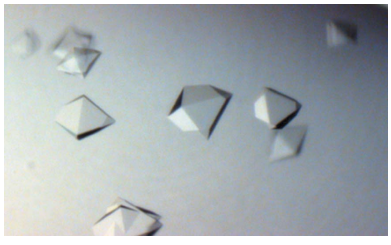

mutations sequentially near the conserved active-site motifs with antibiotic resistance (Sanbongi *et al.*, 2004). They reported that mutated PBP 2Bs usually increase the penicillin and carbapenem minimum inhibitory concentrations (MICs) necessary to inhibit bacterial growth, whereas mutated PBP 2Xs most often increase the cephalosporin MICs. They also reported that when PBP 1A mutants coexisted in strains with PBP 2B and/or PBP 2X mutants, the relevant MIC levels were further increased. Reichmann and colleagues had previously performed a similar survey using a much smaller number of β-lactam-resistant strains; their findings were similar to those of Sanbongi and colleagues (Reichmann *et al.*, 1996).

S. pneumoniae PBP 2B contains a short cytoplasmic region, a transmembrane region and a periplasmic unit consisting of two domains: the N-terminal and transpeptidase domains. The transpeptidase domain is the crystallization subject of this paper. This transpeptidase domain includes the conserved sequence motifs Ser391-Val392-Val393-Lys394 (S*XX*K), Ser448-Ser449-Asn450 (S*X*N) and Lys620-Thr621-Gly622 (KT/SG). (The residue numbering is that of GenPept accession No. NP_359110.) The mutations Thr431Lys, Gln432Leu, Thr451Ala and Ala624Gly, which are sequentially near two of the conserved motifs, were found in two or more of the *pbp2b* genes sequenced by Sanbongi *et al.* (2004). When the Thr451Ala mutation was introduced into a recombinant soluble form of a PBP 2B from the penicillin-susceptible *S. pneumoniae* R6 strain, it decreased the original affinity of the protein for penicillin G by 60% (Pagliero *et al.*, 2004). The binding affinities of various *S. pneumoniae* PBP 2B mutant transpeptidases have been measured for four carbapenem antibiotics: imipenem, panipenem, biapenem and meropenem (Baba *et al.*, 2003). The mutated transpeptidases contained the single mutations Ala624Gly or Thr451Ala, the double mutation Thr431Lys/Gln432Leu or combinations of the three. The single and double mutations have little effect on the binding specificities of the carbapenens. However, they are much more effective in combination, especially when Ala624Gly and one or more of the other mutations are present, although the effects are not additive. Additionally, Ala624 seems to be particularly important for the binding of meropenem, whereas Thr431 and/or Gln432 seem to be somewhat important for the binding of imipenem and biapenem. To understand the complicated effects of these PBP 2B mutations, crystal structures of *S. pneumoniae* β-lactam-sensitive and β-lactam-resistant PBP 2Bs are needed.

Crystal structures of soluble or trypsin-digested forms of PBPs 1A, 1B, 2X and 3 obtained from the penicillin-susceptible R6 strain are available (Contreras-Martel *et al.*, 2006; Gordon *et al.*, 2000; Lovering *et al.*, 2006; Macheboeuf *et al.*, 2005; Morlot *et al.*, 2005; Yamada *et al.*, 2007), while no structures are available for PBP 2B. (By definition, soluble PBPs lack the cytoplasmic and transmembrane regions.) Additionally, crystal structures of a trypsin-digested form of PBP 1A and of soluble PBP 2X from penicillin-resistant *S. pneumoniae* strains are also available (Dessen *et al.*, 2001; Job *et al.*, 2008; Pernot *et al.*, 2004). Examination of the various crystal structures of *S. pneumoniae* PBPs 1A and 2X, in conjunction with biochemical characterization of *S. pneumoniae* PBP 1A and 2X mutants, reveals that there are several ways to introduce β-lactam resistance (Carapito *et al.*, 2006; Chesnel *et al.*, 2003; Macheboeuf *et al.*, 2006). For PBP 1A, the mutations Thr371Ala, which is adjacent to the catalytic Ser370, and Thr574Asn/Ser575Thr/Gln576Gly/Phe577Tyr, which is part of a loop bordering the active-site cleft, narrow the active-site cavity and reorient Ser370. For PBP 2X, at least three mechanisms for β-lactam resistance are known. One mechanism involves the mutation Thr338Ala. Residue 338 is adjacent to the catalytic Ser337 and the mutation causes a reorientation of the Ser337 side chain. A second mechanism, involving the mutants Ser389Leu and Asn514His, destabilizes and thereby enlarges the active-site cavity. Consequently, the S*X*N motif, which is part of a loop, moves away from its optimal position in the active site. The mutations Ile371Thr and Arg384Gly also increase the disorder of the S*X*N loop. The third mechanism results from a change in the charge distribution at the entryway to the active-site cavity owing to a Gln552Glu mutation and impedes the entry of negatively charged β-lactams. Conversely, because there are no available crystal structures for *S. pneumoniae* PBP 2B and its β-lactam-resistant mutants, any possible structural alterations conferred by the Thr431Lys, Gln432Leu, Thr451Ala and Ala624Gly mutations are uncharacterized. Additionally, the reason why cephalosporins are only weakly bound to the PBP 2Bs of penicillin-susceptible *S. pneumoniae* strains is not known (Hakenbeck *et al.*, 1987; Pagliero *et al.*, 2004). In order to clarify the aforementioned PBP 2B structure–function relationships and to expedite the rational design of new antibiotics, we have initiated structural studies on the PBP 2B transpeptidase, the first of which is reported here.

A soluble form of *S. pneumoniae* PBP 2B has been expressed and purified (Pagliero *et al.*, 2004). Although we attempted to crystallize soluble PBP 2B and a soluble PBP 2B mutant that contains the Thr431Lys, Gln432Leu, Thr451Ala and Ala624Gly mutations, only low-quality diffraction data to 3.5 Å resolution were obtained using a crystal of the mutant and no diffraction-quality wild-type soluble PBP 2B crystals have been grown to date. We therefore could not solve the structures (unpublished results). As mentioned previously, structures of other *S. pneumoniae* PBPs exist. For PBP 2X, the other hmw class B PBP from the R6 strain, a soluble form was crystallized in two different crystal forms, hexagonal and orthorhombic; the former diffracted to 3.5 Å resolution and the latter to 2.4 Å resolution (Pares *et al.*, 1996; Gordon *et al.*, 2000). However, it took several months for the orthorhombic crystals to grow. In an attempt to improve the quality and growth characteristics of these crystals, soluble PBP 2X was digested with trypsin and the resulting noncovalently associated complex consisting of an N-terminal domain (residues Thr71–Lys238), a transpeptidase domain (residues Leu241–Lys625) and a C-terminal domain (Ala626–Asp750) was crystallized (Yamada *et al.*, 2007). Its structure was solved to 2.6 Å resolution. For the hmw class A *S. pneumoniae* PBPs, trypsin-digested forms of PBPs 1A and 1B also exist and their structures have been solved to 2.6 and 1.9 Å, respectively (Contreras-Martel *et al.*, 2006; Macheboeuf *et al.*, 2005). As with PBP 2X, the trypsin-digest products used in the crystallographic studies are noncovalently bound complexes. Starting at the N-terminus, each of these complexes contains a short peptide derived from the transglycosylase domain (residues Leu47–Arg70 for PBP 1A and Asp101–Arg125 for PBP 1B) and a second chain (residues Ser264–Arg653 for PBP 1A and Gly306–Pro791 for PBP 1B) consisting of a linker sequence that connects the transglycosylase domain to the transpeptidase domain, the transpeptidase domain and a C-terminal extension. However, to date no isolated transpeptidase domain of any hmw PBP from *S. pneumoniae* has been successfully expressed as an active protein (Di Guilmi *et al.*, 1998). Consequently, expression of a soluble PBP followed by trypsin digestion to remove loop regions and/or other domains is a practical strategy.

Here, we report the expression and limited proteolysis of a soluble form of *S. pneumoniae* PBP 2B that produces the transpeptidase domain. The recombinant construct contains the four mutations listed above that are associated with β-lactam resistance as well as two additional mutations, Lys229Gln and Lys561Gln, that prevent trypsin digestion at these sites. We also report the purification, crystallization and preliminary crystallographic analysis of the domain.

2. Materials and methods

2.1. Protein expression and purification

The gene for the soluble form of *S. pneumoniae* R6 PBP 2B (Asn43–Asn685) was amplified by PCR using the forward primer 5′-AGTGGATCCCATATGAACAAGGATTTTTACGAAAA-3′ and the reverse primer 5′-CCCCTCGAGCTAGTTCATTGGATGGTA-TTTTTG-3′. The amplified PCR gene fragment was digested with *Bam*HI and *Xho*I and ligated into a pGEX-4T-1 expression vector (GE Healthcare Biosciences, Piscataway, New Jersey, USA) that carried DNA sequences encoding an N-terminal GST tag with a thrombin-cleavage site at its C-terminus. [The gene encodes a four-residue sequence (Gly-Ser-His-Met) between the thrombin cleavage site and Asn43.] The mutations Thr431Lys, Gln432Leu, Thr451Ala and Ala624Gly were then introduced using a QuikChange Site-Directed Mutagenesis Kit (Stratagene, La Jolla, California, USA). Using the same procedure, the mutations Lys229Gln and Lys561Gln were also introduced. The resulting plasmid was transformed into *Escherichia coli* B834(DE3) (Novagen, Madison, Wisconsin, USA). The cells, which were suspended in 4.8 l LeMaster medium (LeMaster & Richards, 1985) supplemented with 25 µg ml^{-1} SeMet and 100 µg ml^{-1} ampicillin and grown to an OD of 0.5–0.8, were incubated at 303 K for 4 h after protein expression had been induced with 1 m*M* IPTG (final concentration).

Cells were harvested by centrifugation, suspended in 1 m*M* EDTA, 5 m*M* 2-mercaptoethanol, 1 m*M* phenylmethylsulfonyl fluoride (PMSF), 1 µ*M* leupeptin, 1 µ*M* pepstatin A, 0.1 mg ml^{-1} lysozyme, Dulbecco's phosphate-buffered saline that contained neither calcium chloride nor magnesium chloride (PBS; Sigma–Aldrich, St Louis, Missouri, USA) and sonicated and the crude lysate was centrifuged. The supernatant was applied onto a 50 ml glutathione Sepharose 4 Fast Flow column (GE Healthcare Biosciences) equilibrated with 1 m*M* EDTA, 5 m*M* 2-mercaptoethanol, PBS. Proteins that bound glutathione were eluted in 20 m*M* Tris–HCl pH 7.9, 10 m*M* reduced glutathione, 1 m*M* EDTA, 5 m*M* 2-mercaptoethanol and then dialyzed against 20 m*M* Tris–HCl pH 7.9, 1 m*M* EDTA, 5 m*M* 2-mercaptoethanol. The retentate was then digested with a low concentration of trypsin (2.3 µg ml^{-1}; Sigma–Aldrich) for 1 h at 298 K. The reaction was stopped by adding 1 m*M* PMSF (final concentration). This digestion targets the thrombin-cleavage site, removing the GST tag.

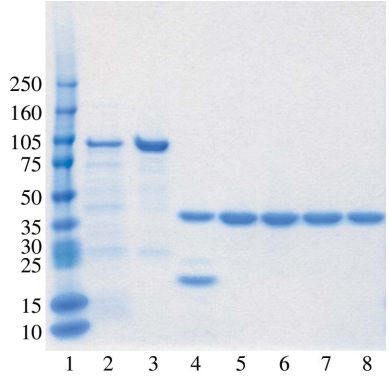

Figure 1
SDS–PAGE analysis. The proteins (0.88 µg) were subjected to SDS–PAGE under reducing conditions. Lane 1, molecular-weight markers (kDa). Lane 2, soluble extract from *E. coli*. Lane 3, proteins that bound to glutathione Sepharose 4. Lane 4, protein products after the 'high-concentration' trypsin digest. Lane 5, proteins of the major peak eluted from MonoQ. Lane 6, pooled flowthrough fractions from Macro-Prep Ceramic Hydroxyapatite. Lane 7, proteins of the major peak eluted from MonoS. Lane 8, purified PBP 2B transpeptidase after Superdex 75 chromatography.

The protein mixture was then applied onto a MonoQ HR10/10 column (GE Healthcare Biosciences) and eluted with a linear gradient of 0–250 m*M* NaCl in 20 m*M* Tris–HCl pH 7.9, 1 m*M* EDTA, 5 m*M* 2-mercaptoethanol. The fractions of the major peak were pooled and dialyzed against 20 m*M* Tris–HCl pH 7.9, 1 m*M* EDTA, 5 m*M* 2-mercaptoethanol. The protein retentate was digested with a high concentration of trypsin (125 µg ml^{-1}) for 1 h at 298 K to produce the PBP 2B transpeptidase domain. The reaction was stopped by adding 1 m*M* PMSF (final concentration). We initially planned to perform only a single trypsin digest to remove the GST tag and then to directly isolate a trypsin-digested form of PBP 2B. However, pilot studies indicated that an excessive amount of trypsin would be needed to accomplish this. The results of the pilot study also indicated that it would be possible to cleave the GST tag with a small amount of trypsin. Thus, the two-step trypsin-digestion procedure was developed. The digest was applied onto a MonoQ HR10/10 column and eluted with a linear gradient of 0–250 m*M* NaCl in 20 m*M* Tris–HCl pH 7.9, 1 m*M* EDTA, 5 m*M* 2-mercaptoethanol. Pooled fractions of the major protein peak were dialyzed against 1 m*M* DTT, 5 m*M* potassium phosphate pH 6.8 and then applied onto a Macro-Prep Ceramic Hydroxyapatite Type I column (Bio-Rad, Hercules, California, USA). The flowthrough fractions were pooled, dialyzed against 50 m*M* sodium acetate pH 5.0, 1 m*M* EDTA, 1 m*M* DTT, applied onto a MonoS HR10/10 column (GE Healthcare Biosciences) and eluted with a linear gradient of 0–200 m*M* NaCl in the same buffer. The fractions of the major protein peak were concentrated and loaded onto a HiLoad 16/60 Superdex 75 prep-grade size-exclusion column (GE Healthcare Biosciences) equilibrated with 20 m*M* Tris–HCl pH 7.9, 150 m*M* NaCl, 1 m*M* EDTA, 1 m*M* DTT. The fractions of the major protein peak were pooled, diluted into 10 m*M* Tris–HCl pH 7.9, 50 m*M* NaCl, 0.33 m*M* EDTA, 1 m*M* DTT and concentrated to a final protein concentration of 4.7 mg ml^{-1}. An electrospray ionization mass spectrum of the purified protein was recorded using a Waters ZQ mass spectrometer (Waters Corp., Milford, Massachusetts, USA). The spectrum was processed with *MaxEnt* 1 from the *MassLynx* software package (Waters Corp.). An average molecular mass for the protein was calculated using the molecular masses of several different charge states.

2.2. Crystallization

Crystallization conditions were screened by the sparse-matrix technique (Jancarik & Kim, 1991) using the components of Structure Screens 1 and 2 (Molecular Dimensions, Apopka, Florida, USA) and JBScreen Classics 2, 3, 5 and 6 (Jena Bioscience, Jena, Germany) kits supplemented with 10 m*M* DTT. All crystallization trials were set up manually and used sitting-drop vapour diffusion at 293 K. For each screen, 0.4 µl protein solution (4.7 mg ml^{-1}) was mixed with an equal volume of reservoir solution and equilibrated against 100 µl reservoir solution. We found that diffraction-quality crystals were obtained within a few days when a reservoir solution consisting of 1.5 *M* ammonium sulfate, 15%(*w*/*v*) glycerol, 0.1 *M* Tris–HCl pH 8.5, 10 m*M* DTT (JBScreen Classic 6 condition No. B1) was used. Crystals obtained from the initial screen were used for data collection.

2.3. Data collection and phasing

A crystal was transferred to 2 µl reservoir solution and the glycerol concentration was then increased by adding 2 µl 1.6 *M* ammonium sulfate, 25%(*w*/*v*) glycerol, 10 m*M* DTT, 0.1 *M* Tris–HCl pH 8.5 to the drop and removing the same volume from the drop after mixing. This concentration procedure was repeated six times. The crystal was then

flash-cooled in a cryostream of N_2 gas at 103 K. A multiple-wavelength anomalous dispersion (MAD) data set was collected at wavelengths of 0.90000 Å (high-energy remote), 0.97907 Å (peak) and 0.97948 Å (edge) at 100 K on the pharmaceutical industry beamline (BL32B2) at the SPring-8 synchrotron facility (Hyogo, Japan) using an R-AXIS V detector (Rigaku Co., Tokyo, Japan). 40 rotation images at each wavelength were collected with an oscillation angle of 1° and an exposure time of 50 s for each image. All diffraction data were integrated and scaled using *CrystalClear* (Rigaku Co.). The positions of the Se atoms were determined using *SOLVE* (Terwilliger & Berendzen, 1999). Density modification was performed with *RESOLVE* (Terwilliger, 2000).

3. Results and discussion

SDS–PAGE analysis shows that the molecular weight of the purified trypsin-digested PBP 2B fragment is consistent with that expected for the transpeptidase domain (Leu315–Asn685; Fig. 1). The molecular weight and therefore the identity of the fragment were verified by electrospray ionization mass spectrometry. The measured molecular weight of the protein is 39 851 Da, which is in good agreement with the calculated molecular weight of 39 843 Da for the protein when all of the methionines are replaced with selenomethionines. The DNA sequence and amino-acid sequence were deposited in the DDBJ/EMBL/GenBank database under accession No. AB378087.

Initially, we attempted to isolate a transpeptidase domain containing only the four mutations associated with β-lactam resistance. We found that when the soluble form of PBP 2B was digested with trypsin, four fragments, Gly66–Arg228, Gly66–Lys229, Gly562–Gln680 and the desired transpeptidase domain Leu315–Asn685, accumulated to identifiable levels (unpublished results). The fragment Gly562–Gln680 lacks two of three conserved sequence motifs found in the transpeptidase and therefore must be inactive. To prevent the production of this undesirable fragment, we introduced the mutation Lys561Gln.

As mentioned above, a limited trypsin digestion of soluble PBP 2X produces a protein composed of three noncovalently associated fragments: residues 71–238 (the N-terminal domain), 241–625 (the transpeptidase domain) and 626–750 (the C-terminal domain) (Yamada *et al.*, 2007). Rather than chance the occurrence of similar PBP 2B species, *i.e.* a mixture of noncovalently bound 66–228/229 transpeptidase species, before further developing the purification protocol we reconstructed the *pbp2b* gene and introduced the mutation Lys229Gln to circumvent trypsin cleavage at least at this position. In other words, even if the transpeptidase domain and the N-terminal domain of soluble PBP 2B were to co-purify, as do those of PBP 2X, the purified product would be homogeneous because only one N-terminal fragment, residues 66–228, could exist. However, this mutation proved to be unnecessary. An N-terminal fragment did not co-purify with the transpeptidase (Fig. 1). Therefore, in retrospect, only the Lys561Gln mutation was needed; the mutations at Lys229 (or Arg228) were not. Because the transpeptidase domain of PBP 2B is stable as an isolated domain, which is not the case for the PBP 1A, 1B and 2X domains, cloning and expressing a functional PBP 2B transpeptidase domain may produce active protein.

During the crystallization screening process, crystals were obtained from solutions of ammonium sulfate, magnesium sulfate and lithium sulfate with pH values of 6.5–8.5 (Structure Screen 1 condition Nos. 27, 30 and 32, Structure Screen 2 condition Nos. 7 and 20 and JBScreen Classic 6 condition Nos. A4, A6, B1, B4, B5 and C4). These results suggest that sulfate ions influence the crystal-packing interactions and/or contribute to the stability of the transpeptidase domain. We also tried to find crystallization conditions for a transpeptidase domain that contained only the Lys561Gln mutation and not the four mutations associated with β-lactam resistance. However, we obtained only clusters of thin needle-like crystals that were not suitable for diffraction experiments (unpublished results). Introdu-

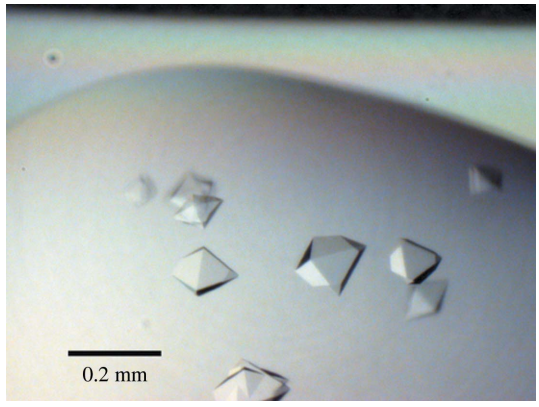

Figure 2
Crystals of the SeMet-substituted transpeptidase domain of PBP 2B.

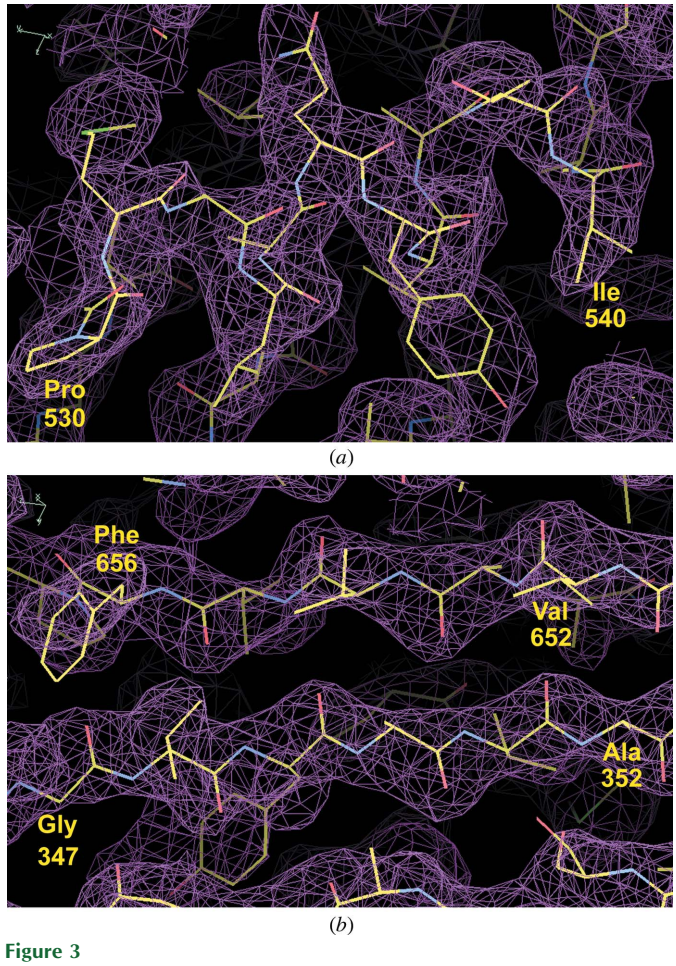

Figure 3
Electron-density maps (contoured at 1.5σ) and the initial atomic model derived from *RESOLVE* calculations (*a*) for an α-helix (residues 530–540) and (*b*) for two β-strands (residues 347–352 and 652–656). C, N, O and Se atoms are coloured yellow, blue, red and green, respectively. This figure was prepared using *Coot* (Emsley & Cowtan, 2004).

Table 1
Data-collection statistics.

Values in parentheses are for the highest resolution shell.

	Remote	Peak	Edge
X-ray source	SPring-8, BL32B2		
Detector	R-AXIS V imaging plate		
Temperature (K)	100		
Space group	$P4_32_12$		
Unit-cell parameters (Å)	$a = b = 86.39$, $c = 143.27$		
Wavelength (Å)	0.90000	0.97907	0.97948
Resolution range (Å)	28–2.4 (2.48–2.40)	28–2.4 (2.48–2.40)	30–2.4 (2.48–2.40)
Total reflections	65067 (6137)	65100 (6101)	64796 (6101)
Unique reflections	35820 (3380)	35622 (3328)	35525 (3338)
$R_{\rm merge}$†	0.054 (0.170)	0.057 (0.188)	0.057 (0.198)
Completeness (%)	88.2 (83.3)	87.7 (82.2)	87.7 (83.1)
$\langle I/\sigma(I)\rangle$	10.4 (4.2)	10.1 (4.0)	9.8 (3.9)
f' (e^-)	−3.50	−7.80	−10.40
f'' (e^-)	2.81	4.11	2.71

† $R_{\rm merge} = \sum_{hkl}\sum_i |I_i(hkl) - \langle I(hkl)\rangle| / \sum_{hkl}\sum_i I_i(hkl)$, where $I_i(hkl)$ is the ith measurement of the intensity of reflection hkl and $\langle I(hkl)\rangle$ is the mean intensity of reflection hkl.

cing the four mutations associated with β-lactam resistance may have caused a conformational change and/or changed the surface environment of the domain, which in turn may have positively influenced the ability of the domain to crystallize.

For the diffraction experiments, bipyramidal crystals (Fig. 2) with average dimensions of approximately 0.1 × 0.1 × 0.1 mm were irradiated. The results found for the processing and scaling of the diffraction data indicated that the space group was either $P4_12_12$ or $P4_32_12$. The asymmetric unit contains one molecule, with a Matthews coefficient $V_{\rm M}$ of 3.39 Å^3 Da^{-1}, corresponding to a solvent content of 63.7%. Both values are within the normal ranges found for protein crystals (Matthews, 1968). As a consequence of radiation damage and/or the formation of ice on the surface of the cryoloop, the MAD data set is less than 90% complete. Nonetheless, initial phases could be obtained using *SOLVE* (Terwilliger & Berendzen, 1999). All of the nine expected Se-atom positions per asymmetric unit were found. The mean figure of merit was 0.33 at this stage of analysis. After density modification using *RESOLVE* (Terwilliger, 2000), the mean figure of merit increased to 0.65. The resulting experimental electron-density map is readily interpretable and an initial model could be built using *RESOLVE* (Terwilliger, 2003*a*,*b*) that accounts for about 80% and 40% of the main-chain and the side-chain atoms, respectively. After calculating electron-density maps using the improved phases obtained from *RESOLVE* for space groups $P4_12_12$ and $P4_32_12$, it was clear that the correct space group is $P4_32_12$ (Fig. 3). Prior to refinement, the initial model yielded an R factor of 47.4% in *REFMAC*5 (Murshudov *et al.*, 1997). Diffraction data statistics are summarized in Table 1. Further model building and structure refinement using this MAD data and additional higher resolution data have been completed and will be reported elsewhere.

We thank Dr Y. Katsuya for help with XAFS spectroscopy and data collection at SPring-8. We thank Ms K. Nagano for technical assistance with protein expression and purification. We also thank Ms K. Maeda for her excellent help with cloning.

References

Baba, N., Kondo, K., Yamada, M., Ida, T. & Ohsawa, F. (2003). *Jpn J. Chemother.* **51**, *Suppl. A*, 90. (In Japanese).
Barcus, V. A., Ghanekar, K., Yeo, M., Coffey, T. J. & Dowson, C. G. (1995). *FEMS Microbiol. Lett.* **126**, 299–303.
Carapito, R., Chesnel, L., Vernet, T. & Zapun, A. (2006). *J. Biol. Chem.* **281**, 1771–1777.
Chesnel, L., Pernot, L., Lemaire, D., Champelovier, D., Croizé, J., Dideberg, O., Vernet, T. & Zapun, A. (2003). *J. Biol. Chem.* **278**, 44448–44456.
Contreras-Martel, C., Job, V., Di Guilmi, A. M., Vernet, T., Dideberg, O. & Dessen, A. (2006). *J. Mol. Biol.* **355**, 684–696.
Dessen, A., Mouz, N., Gordon, E., Hopkins, J. & Dideberg, O. (2001). *J. Biol. Chem.* **276**, 45106–45112.
Di Guilmi, A. M., Mouz, N., Andrieu, J.-P., Hoskins, J., Jaskunas, S. R., Gagnon, J., Dideberg, O. & Vernet, T. (1998). *J. Bacteriol.* **180**, 5652–5659.
Emsley, P. & Cowtan, K. (2004). *Acta Cryst.* D**60**, 2126–2132.
Goffin, C. & Ghuysen, J. M. (1998). *Microbiol. Mol. Biol. Rev.* **62**, 1079–1093.
Gordon, E., Mouz, N., Duée, E. & Dideberg, O. (2000). *J. Mol. Biol.* **299**, 477–485.
Hakenbeck, R., Tornette, S. & Adkinson, N. F. (1987). *J. Gen. Microbiol.* **133**, 755–760.
Jacobs, M. R. (2004). *Am. J. Med.* **117**, *Suppl.* 3*A*, 3S–15S.
Jancarik, J. & Kim, S.-H. (1991). *J. Appl. Cryst.* **24**, 409–411.
Job, V., Carapito, R., Vernet, T., Dessen, A. & Zapun, A. (2008). *J. Biol. Chem.* **283**, 4886–4894.
LeMaster, D. M. & Richards, F. M. (1985). *Biochemistry*, **24**, 7263–7268.
Lovering, A. L., De Castro, L., Lim, D. & Strynadka, N. C. (2006). *Protein Sci.* **15**, 1701–1709.
McDonough, M. A., Anderson, J. W., Silvaggi, N. R., Pratt, R. F., Knox, J. R. & Kelly, J. A. (2002). *J. Mol. Biol.* **322**, 111–122.
Macheboeuf, P., Contreras-Martel, C., Job, V., Dideberg, O. & Dessen, A. (2006). *FEMS Microbiol. Rev.* **30**, 673–691.
Macheboeuf, P., Di Guilmi, A. M., Job, V., Vernet, T., Dideberg, O. & Dessen, A. (2005). *Proc. Natl Acad. Sci. USA*, **102**, 577–582.
Matthews, B. W. (1968). *J. Mol. Biol.* **33**, 491–497.
Morlot, C., Pernot, L., Gouellec, A. L., Di Guilimi, A. M., Vernet, T., Dideberg, O. & Dessen, A. (2005). *J. Biol. Chem.* **280**, 15984–15991.
Murshudov, G. N., Vagin, A. A. & Dodson, E. J. (1997). *Acta Cryst.* D**53**, 240–255.
Pagliero, E., Chesnel, L., Hopkins, J., Croizé, J., Dideberg, O., Vernet, T. & Di Guilmi, A. M. (2004). *Antimicrob. Agents Chemother.* **48**, 1848–1855.
Pares, S., Mouz, N., Pétillot, Y., Hakenbeck, R. & Dideberg, O. (1996). *Nature Struct. Biol.* **3**, 284–289.
Pernot, L., Chesnel, L., Le Gouellec, A., Croizé, J., Vernet, T., Dideberg, O. & Dessen, A. (2004). *J. Biol. Chem.* **279**, 16463–16470.
Reichmann, P., König, A., Marton, A. & Hakenbeck, R. (1996). *Microb. Drug Resist.* **2**, 177–181.
Sanbongi, Y., Ida, T., Ishikawa, M., Osaki, Y., Kataoka, H., Suzuki, T., Kondo, K., Ohsawa, F. & Yonezawa, M. (2004). *Antimicrob. Agents Chemother.* **48**, 2244–2250.
Terwilliger, T. C. (2000). *Acta Cryst.* D**56**, 965–972.
Terwilliger, T. C. (2003*a*). *Acta Cryst.* D**59**, 38–44.
Terwilliger, T. C. (2003*b*). *Acta Cryst.* D**59**, 45–49.
Terwilliger, T. C. & Berendzen, J. (1999). *Acta Cryst.* D**55**, 849–861.
Yamada, M., Watanabe, T., Miyara, T., Baba, N., Saito, J., Takeuchi, Y. & Ohsawa, F. (2007). *Antimicrob. Agents Chemother.* **51**, 3902–3907.